

Recent LISA studies at the University of Colorado

M Nickerson, E Ames, and P L Bender

JILA, University of Colorado and NIST, Boulder, CO 80309-0440, USA

Email: nickermj@jila.colorado.edu

Abstract. We report on LISA experimental projects being pursued at JILA. Our focus is on the design and testing of a flight-compatible laser stabilization reference cavity. This is a dual cylinder ULE cavity, designed to provide high thermal and thermo-mechanical isolation in the millihertz frequency regime of interest to LISA. A modification of this hard-mounted design may allow for use in space without the need for clamping during launch. Progress so far consists of initial design, performance estimates, and construction. Simple thermal model calculations on the design indicate a thermal attenuation of 10^6 at 1 mHz, corresponding to a cavity strain of $3 \cdot 10^{-16}$ /rtHz for a 0.01 K/rtHz stability of the mounting surface. Finite element analysis indicates cavity strain attenuation of $5 \cdot 10^7$ or better due to thermo-mechanical effects in the surrounding environment, and low sensitivity to vibration along the cavity axis. Setup and testing of two identical cavities and a laser-locking test system is ongoing. Another project was recently concluded, testing the low-frequency stability of commercial voltage references. Voltage reference performance is relevant to the stability of electrically applied forces on the LISA proof masses, and commercial references do not have well characterized noise in the sub-Hz regime. Our measurements confirmed that the best commercial reference was the AD587LN, with a typical noise of 2.1 ± 0.6 ppm/rtHz at 0.1 mHz, in a temperature-stabilized environment of ~ 10 mK/rtHz. This agrees closely with prior work by other groups.

1. Introduction

Considering highly stable laser reference cavities used in optical frequency standards, most designs have some sort of soft suspension. For use in space, such designs would need to be clamped down for launch. A fixed-mount cavity design obviates the need for a clamp system, reducing the overall complexity. Prior work has indicated that fixed, center supported cavities can be competitive with standard suspension designs [1]. Building on this work, we have developed a dual-cylinder cavity design that improves thermal isolation, while providing a center support to minimize vibrational disturbances along the axis. The aim of this design is to demonstrate the possibility of a flight-compatible cavity that provides high stability in the millihertz regime of interest to LISA. Progress so far in this project has consisted of the design and construction of two dual-cylinder cavities, and their support structures and vacuum chambers. The cavity design and performance estimates are presented.

2. Reference cavity design

2.1. Cavity construction

The laser reference cavity itself consists of two concentric cylinders and a connecting support disk, formed of a single contiguous piece of ULE. Both cylinders are 100 mm in length; the inner cylinder has a 10 mm ID and 30 mm OD, and the outer cylinder has a 50 mm ID and 70 mm OD. The 5 mm

disk supporting the inner cylinder is vertically centered. A cutaway view of the cavity is shown in figure 1.

The inner cylinder forms the Fabry-Perot spacer, with optically contacted mirrors. It is centrally supported by the connecting disk, which provides symmetry along the cavity axis. For any acceleration along the axis, the change in length caused by the elastic deformation of one half of the cavity is compensated by a correspondingly opposite change in length of the other half. This provides a common-mode rejection of along-axis disturbances, which is the motivation for this support scheme. Thus, the outer cylinder can be firmly mounted to a lab surface, and the effect of any vibration of the surface will be strongly reduced.

The outer cylinder provides support for the connecting disk, and creates a stable environment for the inner cylinder. Any thermal changes must diffuse through the outer cylinder before affecting the Fabry-Perot cavity. Additionally, it serves as a mechanically isolating stage. ULE endcaps are epoxied to each end of the outer cylinder, to further isolate the inner cylinder from thermal disturbances.

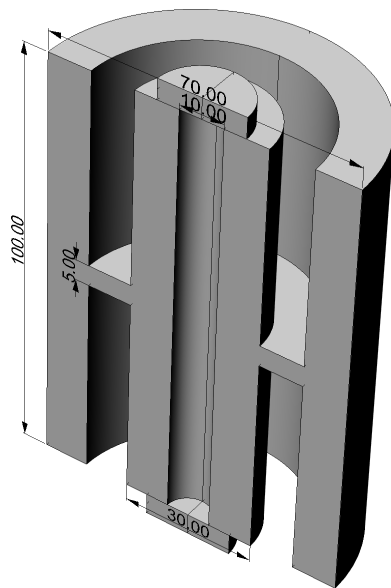


Figure 1. A cutaway view of the laser reference cavity. The inner cylinder forms the Fabry-Perot spacer.

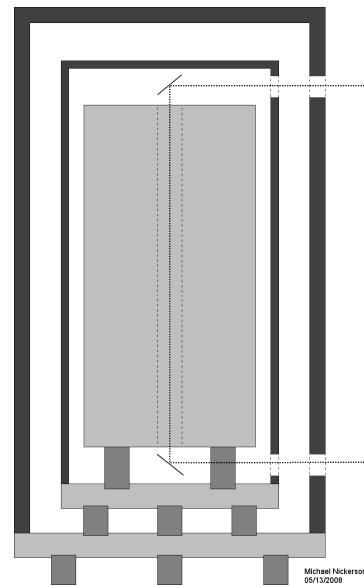


Figure 2. A diagram of the reference cavity and isolation platform. The lowermost legs rest on the vacuum chamber floor.

2.2. Cavity mounting

The laser reference cavity is mounted on a 55 mm high isolation platform, designed to provide thermal and thermo-mechanical isolation. The platform consists of three stages of 10 mm diameter ULE legs, separated by 10 mm thick Zerodur disks. The legs are attached to the disks and the lower cavity endcap with epoxy, and the lowermost set of legs rests on the floor of a vacuum chamber. Two aluminum thermal shields rest on the Zerodur disks, providing radiation shielding for the reference cavity. A diagram of this mounting scheme is shown in figure 2.

The three-stage platform results in significant thermal decoupling from the floor of the vacuum chamber, improving the thermal stability of the cavity. The series of legs also provides thermo-mechanical isolation, flexing to reduce thermally-induced strain changes in the vacuum chamber floor. The consistent use of low-expansion materials minimizes the thermo-mechanical contribution of the support structure itself.

3. Reference cavity performance estimates

3.1. Vibration isolation

Vibration performance estimates were developed using finite element analysis. To determine the cavity strain due to vibration, the cavity, endcaps, and upper mount legs were modeled with accurate dimensions and material properties. The upper mount legs were placed on 1 cm² blocks, which were given an upward acceleration. A high resolution FEA was then run, simulating the response of the system. An example result is shown in figure 3. Cavity strain was determined by averaging displacement over the inner cylinder's mirror surfaces.

Results of this finite element analysis indicate that the lengthwise strain on the Fabry-Perot cavity will be under 2×10^{-12} for a 1 m/s² acceleration along the cavity axis. This agrees well with preliminary calculations that were performed by T Rosenband of NIST.

Prior to design finalization, Rosenband also ran a series of similar tests to determine the effect of altering the vertical position of the connecting disk. As a result of this, the final design offsets the disk from the center by 190 microns. More detailed simulations agree with Rosenband's result to within manufacturing tolerances; the cavity strain due to vertical acceleration is minimized with a disk offset of ~ 0.20 mm.

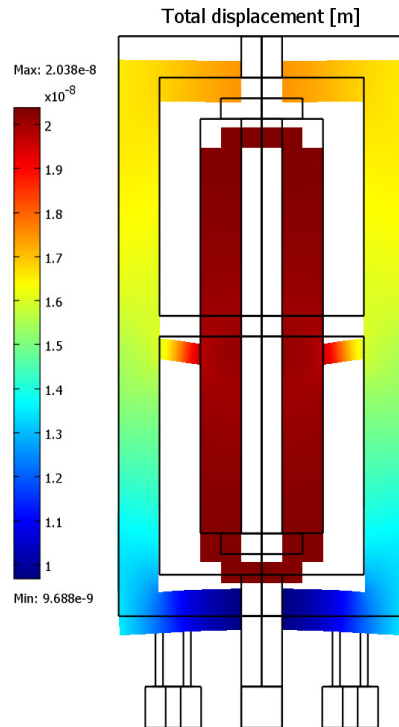


Figure 3. A slice of the laser cavity and upper stage mount, showing the relative displacement for a 1g vertical acceleration. The cavity length strain here is 1.4×10^{-11} .

3.2. Thermo-mechanical isolation

Performance estimates of the thermo-mechanical isolation provided by the mounting system and outer cylinder were also determined using finite element analysis. Due to computation resource limitations, this was done in two stages, and only provides a lower limit on the isolation. The three-stage mounting system was first modelled without the cavity. A radial displacement was applied to the feet of the lowermost legs, simulating thermal expansion of the vacuum chamber floor. Running the FEA then determined the radial displacement at the base of the uppermost legs of the mounting system. A new system consisting of the uppermost legs and full cavity was then modelled. The radial displacement determined from the first simulation was applied to the base of the upper legs, and the cavity response simulated.

The results of this pair of simulations indicate that the cavity strain will be less than $2 \cdot 10^{-8}$ that of any thermally induced strain at the base of the mounting system, i.e. a strain attenuation of $5 \cdot 10^7$ or better from the base of the mounting system to the cavity length. Actual performance is likely to be better than this due to several factors. The simulation overestimates the movement of the uppermost legs, as the stiffness of the cavity is not present when determining the first stage simulation. An additional strain-attenuation factor of ~ 20 may also be present, due to the epoxy connections between the legs, disks, and endcap. Preliminary simulations indicate that there is a factor of ~ 2.5 strain attenuation across each pair of connections due to the presence of a 0.2 mm thick layer of epoxy. This has not been tested extensively, but indicates that the epoxy connections will have some beneficial contribution.

3.3. Thermal isolation

Estimates of the thermal isolation were developed using a simple thermal time constant approach. Assuming that the surfaces of the cavity are uncoated ULE, the thermal time constant for the inner cylinder responding to uniform changes in temperature of the outer cylinder is roughly 800 s. There are comparable contributions from radiation and conduction. At 1 mHz, this gives an attenuation factor of 5.

Assuming an emissivity of 0.05 for the aluminum thermal shields, and a high emissivity of the vacuum chamber, the time constants due to radiative coupling are estimated to be 25000 s from the vacuum chamber wall to the outer radiation shield, 60000 s between the thermal shields, and 58000 s from the inner thermal shield to the outer ULE cylinder. At 1 mHz, the total thermal attenuation through this path is $2 \cdot 10^7$.

The conduction path from the vacuum chamber to the outer cylinder is considered as three steps in series. From the vacuum chamber to the lower disk through 3 legs has an estimated time constant of 3800 s; from the lower disk to the upper disk through 3 legs is 2400 s; and from the upper disk to the center of the outer cylinder through 3 legs and half of the outer cylinder is 31000 s. Thus the overall attenuation of the conductive path at 1 mHz is $2.2 \cdot 10^5$. This is the dominant transfer mechanism by two orders of magnitude, so the radiative transfer path can be neglected.

The product of the attenuation factors from the conduction path to the outer cylinder and then between the two cylinders is $1.1 \cdot 10^6$. For a thermal fluctuation on the floor of the vacuum chamber of 10 mK/rtHz, and the known $3 \cdot 10^{-8}/\text{K}$ ULE thermal expansion coefficient, the estimated cavity strain is only $3.3 \cdot 10^{-16}/\text{rtHz}$ at 1 mHz. The model used to make this estimate is crude, but the results are encouraging.

4. Voltage reference stability

One limit to the stability of electrically applied forces on the LISA proof masses is the noise of onboard voltage references in the relevant frequency range. Commercial voltage references do not have well characterized noise at low frequencies, and thus warrant investigation. We recently concluded a low-frequency performance investigation of a variety of references. The results from this study supplement earlier work done by Heinzl et al. in 2006 [2].

Noise spectra were obtained by running a pair of voltage references through a differential amplifier, and recording this output for analysis. Moderate temperature control ($\sim 10\text{mK}/\text{rtHz}$) was applied to the references and amplifiers. Of the potential external noise sources, the differential amplifier was found to have under a 7% contribution to the overall noise. The measurement circuit and power supply were found to have similarly low noise contributions. Temperature correlation was also determined to be under 10^{-6} V/K, negligible in this case.

Many voltage references were tested, but four performed significantly better than the rest, and were selected for more detailed examination: the AD587LN, LT1021, MAX6126, and LT1236 references. Table 1 and figure 5 present the results of this analysis, giving the stability and a typical spectrum for the four chosen references. The best performer was the AD587LN, with a relative stability of $2.1 \pm 0.6 \text{ ppm}/\text{rtHz}$ at 0.1 mHz [3]. These results are consistent with those obtained by Heinzl et al [2].

Table 1. Relative noise levels of several commercial voltage references at 0.1 mHz.

Voltage Reference	Output Voltage (V)	Noise Level (<i>ppm</i> /rtHz)
AD587LN	10	2.1 ± 0.6
LT1021	5	7.5 ± 1.1
MAX6162	5	5.3 ± 1.5
LT1236	10	6.6 ± 2.2

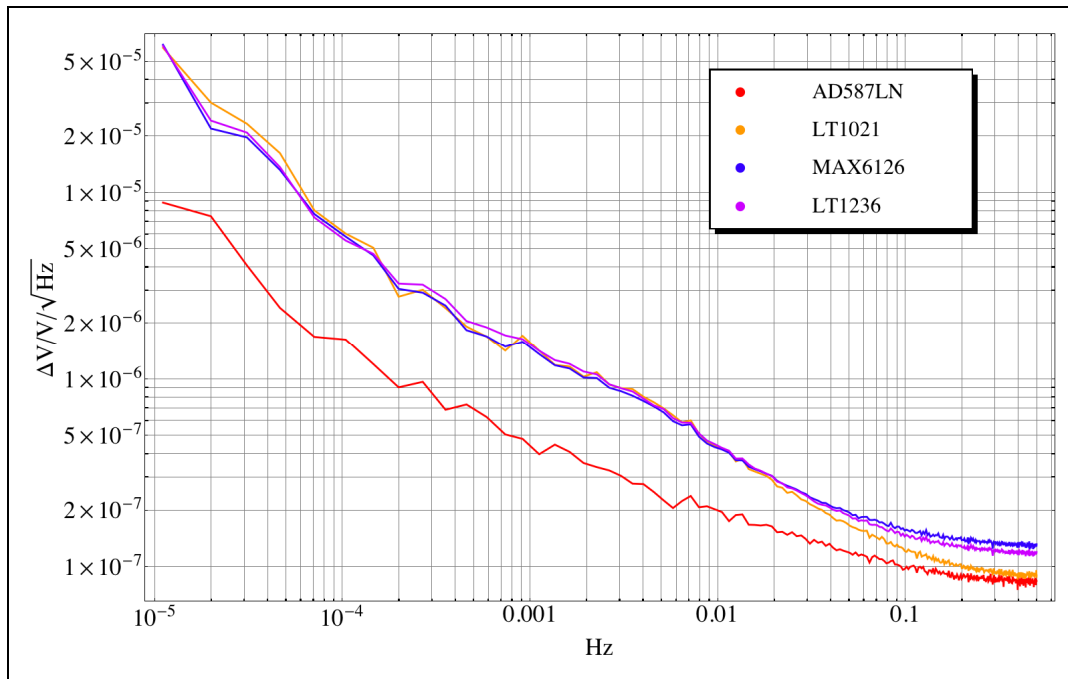


Figure 5. Typical noise spectrum of the AD587LN (lower line), LT1021, MAX6126, and LT1236 voltage references. The vertical axis is fractional noise level per rtHz.

Acknowledgements

Funding for this work was provided by NASA under NASA agreements NNG05GH33G, NGT-50451, NNG06GB73G, and NNX08AB62B. It is a pleasure to thank the following: T. Rosenband for preliminary cavity performance calculations during the design phase; J. L. Hall for insight regarding cavity design and performance, technical guidance during construction, and assistance with the laser setup; M. Notcutt and R. Lalezari for advice on the cavity design; C. D. Hamley for his contributions to the early parts of this work; and D. B. Pinegar for information on low-noise voltage references.

References

- [1] M. Notcutt, L.-S. Ma, J. Ye, and J. L. Hall, *Opt. Lett.* 30, 1815 (2005).
- [2] Heinzl et al., *AIP Conf. Proc.* 873, Laser Interferometer Space Antenna, 6th Int. LISA Symp., S. Merkowitz, J. Livas, 291-296 (2006).
- [3] Ellery Ames, *Characterization of Voltage Reference Noise for the Laser Interferometer Space Antenna*, Honors Thesis, Univ. of Colorado (2008).